In Situ Loading of Cu₂O Nanoparticles on a Hydroxyl Group Rich TiO₂ Precursor as an Excellent Catalyst for the Ullmann Reaction

Fang Niu[1,2], Yan Jiang[1,2], and Weiguo Song[1] (✉)

[1] Beijing National Laboratory for Molecular Sciences (BNLMS); Laboratory for Molecular Nanostructures and Nanotechnology, Institute of Chemistry, Chinese Academy of Sciences, Beijing 100190, China
[2] The Graduate University of the Chinese Academy of Sciences, Yuquanlu, Beijing, 100049,China

ABSTRACT

An *in situ* method has been used to load Cu₂O nanoparticles on the surface of a hydroxyl group rich TiO₂ precursor. Cu₂O nanoparticles are formed by *in situ* reduction of Cu(OH)₂ with Sn²⁺ ions linked to the surface of the TiO₂ precursor. The initial Cu₂O nanoparticles serve as seeds for subsequent particle growth. The resulting Cu₂O nanoparticles are evenly dispersed on the surface of the TiO₂ precursor, and are heat and air stable. The as-prepared composite is an excellent catalyst for Ullmann type cross coupling reactions of aryl halides with phenol. The composite catalyst also showed good stability, remaining highly active after five consecutive runs.

1. Introduction

Nanocatalysis is an important part of nanoscience, materials science and chemistry [1–4]. Many nanoparticles have been used to catalyze a variety of chemical reactions. In many cases, nanoparticles are loaded on the surface of solid supports to form heterogeneous catalysts since this facilitates catalyst recovery [5]. In addition, in several cases, the strong synergistic interaction between nanoparticles and solid supports can greatly enhance the catalytic activity and selectivity [6, 7]. Recently, Cu₂O has attracted great research interest by virtue of its applications in solar energy conversion and catalysis [8–11]. For example, Kim et al. synthesized thermally and air stable Cu₂O nanocubes and used them to catalyze cross coupling of aryl halides with phenols via Ullmann coupling [12].

Son et al. found that Cu₂O coated Cu nanoparticles were an effective catalyst for Ullmann-type amination coupling reactions of aryl chlorides [13]. Many Cu₂O materials with various morphologies, including nanocubes [14–16], nanospheres [17, 18], nanoparticles [19], as well as core–shell nanocomposites [20], have been successfully fabricated. Generally, Cu₂O nanoparticles have higher catalytic activity than the bulk Cu₂O. However, long chain ligands are usually needed to protect the Cu₂O nanoparticles in solution [19], and thus it is rational to load pure Cu₂O nanoparticles onto a support—since protecting ligands are then no longer required—in order to achieve the best catalytic results.

We have previously reported [21] an *in situ* method to load pure noble metals (Pd, Au, Ag, and Pt) nanoparticles onto hydroxyl group rich TiO₂ precursor spheres. The noble metal nanoparticles are very small

---

Address correspondence to wsong@iccas.ac.cn

and are highly dispersed on the TiO_2 precursor surface. The small size coupled with evenly-dispersed manner of the noble metal nanoparticles on the TiO_2 precursor surface make them very active in Suzuki cross coupling reactions. In this study, we extend the method to the loading of Cu_2O nanoparticles on the TiO_2 precursor surface. The Cu_2O nanoparticles have an average size of 3 nm, and are strongly attached to the TiO_2 precursor surface. The highly dispersed Cu_2O nanoparticles on the TiO_2 precursor surface are free of protective ligands and show high catalytic activity for Ullmann type cross coupling reaction of aryl halides with phenol.

2. Experimental

2.1 Synthesis of the TiO₂ precursor

The TiO_2 precursor was synthesized according to the reported method [22]. In a typical experiment, 2 mL of tetrabutoxytitanium was added to 50 mL of ethylene glycol and the mixture was magnetically stirred for 8 h at room temperature. It was then poured into a mixture of 170 mL of acetone and 2.7 mL of water and the resulting suspension stirred for 1 h. The white precipitate was collected by centrifugation, washed five times with ethanol and finally dried at 60 ℃ in an oven.

2.2 Synthesis of the TiO₂ precursor–Cu₂O composite

For the synthesis of TiO_2 precursor–Cu_2O composite with a loading of 7.76 wt% Cu_2O, 100 mg of TiO_2 precursor spheres was dispersed into 20 mL of distilled water, and denoted A. 100 mg of $SnCl_2 \cdot 2H_2O$ was dissolved in 20 mL of HCl (0.02 mol/L) solution, and denoted B. A and B were mixed together with stirring, and the color of the mixture immediately turned yellow. Ten minutes later, the precipitate was recovered by centrifugation and washed five times with distilled water. The recovered yellow precipitate was dispersed into 40 mL of distilled water, forming a milky yellow colloidal mixture. Then, 1 mL of 0.1 mol/L $CuCl_2$ solution was added to the above mixture. Ten minutes later, 2 mL of 0.5 mol/L NaOH solution was added into the mixture and the color of the solution immediately turned to yellowish-green. After another ten minutes,

1 mL of 0.1 mol/L $N_2H_4 \cdot H_2O$ solution was added and the color of the mixture turned to orange. The composite was then aged for ten minutes under magnetic stirring and recovered by centrifugation, followed by washing five times with distilled water. The precipitate was finally dried at 60 ℃ for 12 h under vacuum. TiO_2 precursor–Cu_2O composites with 3.46 wt%, 14.4 wt%, and 29.7 wt% loadings of Cu_2O were also prepared by changing the amounts of the $CuCl_2$, NaOH, and $N_2H_4 \cdot H_2O$ solutions which were added.

2.3 Characterization

The as-prepared composites were characterized by transmission electron microscopy (TEM; JEM JEOL-1011) and high resolution TEM (HRTEM; Tecnai G2 F20 with an energy dispersive X-ray (EDX) system), X-ray diffraction (XRD, D/max-2500), and X-ray photo-electron spectroscopy (XPS, VG ESCALAB 220i-XL). Inductively coupled plasma emission spectrometry (ICP, Shimadzu ICPE-9000) was employed to measure the Cu_2O content of the composite.

2.4 Cross coupling reaction of aryl halides with phenol

The as-prepared TiO_2 precursor–Cu_2O composites were used to catalyze the C–O bond formation reaction between phenol and iodobenzene. In a typical procedure, 92 mg of TiO_2 precursor–Cu_2O composites with 7.76 wt% Cu_2O loading, i.e., 7.2 mg (0.05 mmol) of Cu_2O nanoparticles, 1 mmol of iodobenzene, 1.2 mmol of phenol, 0.25 mmol of biphenyl (as the internal standard compound for GC analysis), and 2.4 mmol of KOH were added to 5 mL of DMF under magnetic stirring. After refluxing for 6 h at 150 ℃, the solid and liquid were separated by centrifugation and the liquid was analyzed by an Agilent 6890 GC with a flame ionization detector (FID) and a 30 m capillary column. In control experiments, various solvents, bases, aryl halides, and Cu_2O catalysts were used to carry out this reaction. The amount of Cu_2O (0.05 mmol, 5 mol%) was kept constant in all of these control experiments. A time dependent experiment using TiO_2 precursor–Cu_2O composites with different Cu_2O loadings was carried out in the same manner as the above experiment. Aliquots of the reaction mixture were collected at specific times during the reaction, and the solid and

liquid were then quickly separated by centrifugation. The liquid was analyzed by GC to measure the reaction yields at specific times.

3. Results and discussion

Scheme 1 depicts the overall procedure for loading Cu_2O nanoparticles on the surface of the TiO_2 precursor. Sn^{2+} is first linked to the TiO_2 surface through the interaction between Sn^{2+} and surface hydroxyl groups. This linkage is achieved by impregnating the TiO_2 precursor with a solution of $SnCl_2 \cdot A Cu(OH)_2$ colloid is formed by adding $CuCl_2$ and NaOH to the solution of the TiO_2 precursor and the surface-linked Sn^{2+} ions reduce the $Cu(OH)_2$ colloid *in situ*. The Cu_2O species initially formed on the TiO_2 precursor are very small and strongly attached on the surface of the TiO_2 precursor. $N_2H_4 \cdot H_2O$ solution was then added to the mixture to reduce the remainder of the $Cu(OH)_2$ colloid to form Cu_2O nanoparticles. The initial Cu_2O species serve as seeds and the Cu_2O formed subsequently attached to the initial seeds to form larger Cu_2O nanoparticles.

Figure 1(a) shows the TEM image of the TiO_2 precursor spheres prepared according to the reported method [22]. Nearly monodisperse spheres with a diameter of about 150 nm were obtained. A large number of hydroxyl groups are present on the surface of the TiO_2 precursor spheres. The presence of these hydroxyl groups was confirmed by FTIR in our previous work [21]. A TEM image of the TiO_2 precursor–Cu_2O composite (with 7.76 wt% of Cu_2O) can be seen in Fig. 1(b). Compared to the smooth surface of the TiO_2 precursor spheres, the surface of the TiO_2 precursor–Cu_2O composite spheres became rough, and numerous Cu_2O nanoparticles can be seen attached on the surface of the TiO_2 precursor–Cu_2O composite spheres. Figure 1(c) shows a HRTEM image of a TiO_2 precursor–Cu_2O composite sphere, showing Cu_2O nanoparticles with an average size of about 3 nm dispersed uniformly on the surface of the TiO_2 precursor. A representative magnified HRTEM image of a Cu_2O nanoparticle (the particle in the red circle in Fig. 1(c)) is shown in the inset of Fig. 1(c). Lattice fringes are clearly visible, with a spacing of 0.303 nm, which corresponds to the lattice spacing of Cu_2O (110) planes. The XRD patterns are shown in Fig. 1(d). There is no XRD signal from the TiO_2 precursor, indicating its amorphous nature. All the peaks in the XRD pattern of the TiO_2 precursor–Cu_2O composite can be indexed as the primitive cubic phase (mineral name: cuprite, JCPDS card file no 77-0199) of Cu_2O.
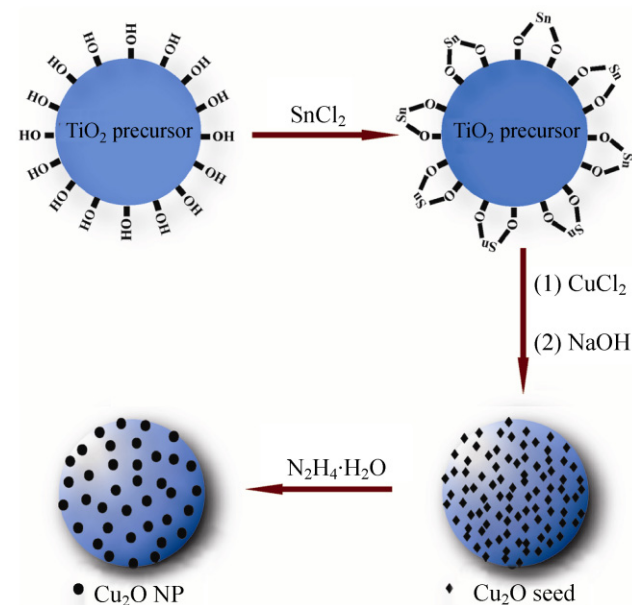
Scheme 1 Schematic procedure for loading Cu_2O nanoparticles on the surface of TiO_2 precursor
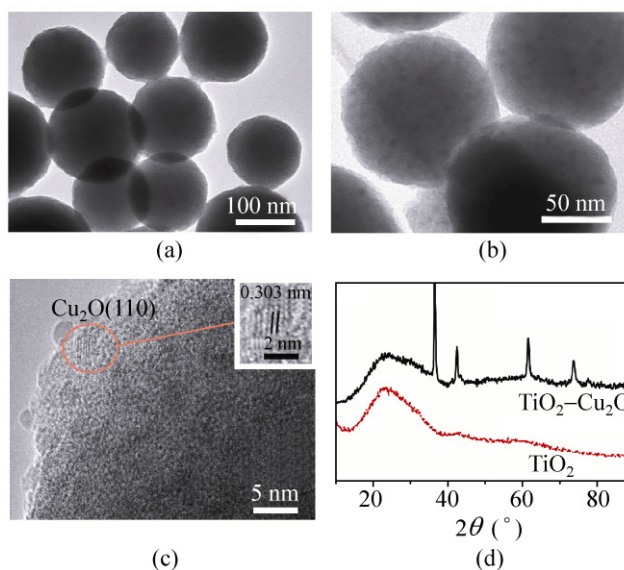
Figure 1 TEM image of the (a) TiO_2 precursor spheres and (b) TiO_2 precursor–Cu_2O composite (with 7.76 wt% of Cu_2O). (c) HRTEM image of the TiO_2 precursor–Cu_2O composite sphere. The insert in (c) is the HRTEM of a Cu_2O nanoparticle coated on the TiO_2 precursor surface. (d) XRD patterns of the TiO_2 precursor and TiO_2 precursor–Cu_2O composite

The pretreatment with Sn^{2+} is crucial for the preparation of the TiO_2 precursor–Cu_2O composite. The Sn^{2+} linked on the surface of the TiO_2 precursor spheres induces the initial formation of the Cu_2O species which can act as seeds for the subsequent growth of Cu_2O nanoparticles. In a control experiment, without pretreatment by $SnCl_2$, solutions of $CuCl_2$, NaOH, and $N_2H_4·H_2O$ were successively added to the TiO_2 precursor colloid solution and mixed for ten minutes. A TEM image of the resulting product (Fig. 2) shows that most of the Cu_2O nanoparticles are not deposited on the surface of the TiO_2 precursor sphere. This indicates that pretreatment by $SnCl_2$ is vital for the successful loading of Cu_2O nanoparticles onto the surface of the TiO_2 precursor and that the Sn^{2+} linkage provides a strong anchor on the surface for the initially formed Cu_2O species.

The as-prepared TiO_2 precursor–Cu_2O composite (with 7.76 wt% of Cu_2O) was also studied by XPS and EDX analysis (Fig. 3). The XPS spectra of the TiO_2 precursor–Cu_2O composite verify the presence of Cu, C, O, and Ti elements as shown in Fig. 3(a). As expected, Sn atoms are only present in the TiO_2 precursor–Cu_2O composite formed with pretreatment by $SnCl_2$. For EDX analysis, we obtained the elemental mappings of Cu, C, Ti, O, and Sn for the TiO_2 precursor–Cu_2O composite sphere prepared with pretreatment by $SnCl_2$. For the TiO_2 precursor–Cu_2O composite sphere indicated in Fig. 3(b), the C, O, Sn, Ti, and Cu elements are evenly distributed on the sphere. The C around the sphere is from the carbon support film on the copper grid for TEM study. Cu is
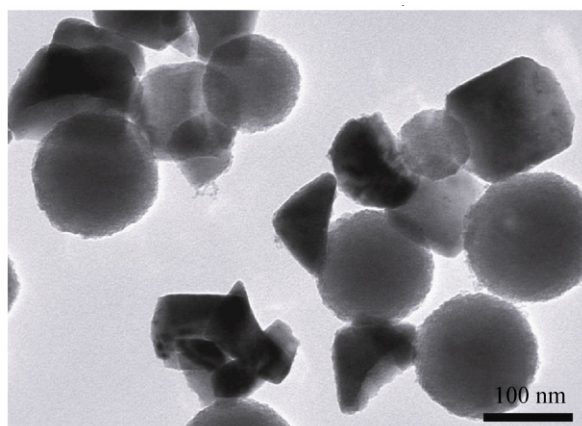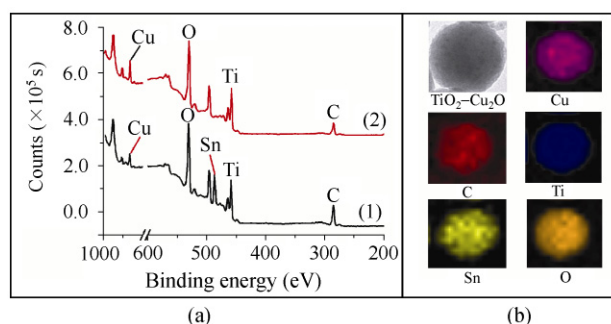
Figure 3 (a) XPS pattern of the as-prepared TiO_2 precursor–Cu_2O composite (1) with pretreatment by $SnCl_2$ and (2) without pretreatment by $SnCl_2$. (b) EDX elemental mapping of the TiO_2 precursor–Cu_2O composite formed with pretreatment by $SnCl_2$

well distributed on the surface with a high dispersion, consistent with the earlier data.

Besides the 7.76 wt% Cu_2O loaded TiO_2 precursor–Cu_2O composite, we also prepared TiO_2 precursor–Cu_2O composites with 3.46 wt%, 14.4 wt%, and 29.7 wt% loadings of Cu_2O. The preparation procedures were the same as for the sample with 7.76 wt% of Cu_2O, except that the concentrations of the added $CuCl_2$, NaOH, and $N_2H_4·H_2O$ solution were adjusted accordingly. TEM images of these three samples are shown in Fig. 4. The Cu_2O species on the surface of the TiO_2 precursor–Cu_2O composite spheres with 3.46 wt% of Cu_2O are too small in size and hardly recognizable, as shown in Fig. 4(a). The sizes of the Cu_2O nanoparticles become larger with increasing Cu_2O loadings. Figure 4(b) shows a TEM image of the TiO_2 precursor–Cu_2O composite spheres with 14.4 wt% of Cu_2O. The Cu_2O nanoparticles are still highly dispersed on the surface of the TiO_2 precursor, with an average size of about 10 nm. When the Cu_2O loading was increased to 29.4 wt%, the Cu_2O nanoparticles became larger and some of them broke away from surface of the TiO_2 precursor (Fig. 4(c)). In this case, presumably, the initially formed Cu_2O seeds were no longer able to anchor all of the Cu_2O on the surface of the TiO_2 precursor spheres.
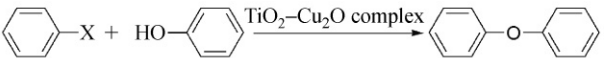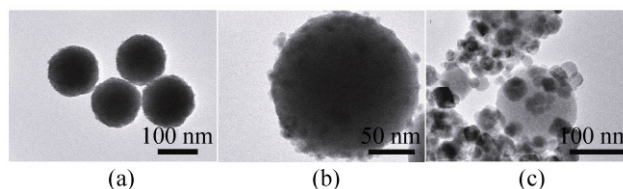
Figure 2 TEM image of the TiO_2 precursor–Cu_2O prepared without pretreatment by $SnCl_2$

Figure 4 TEM images of TiO_2 precursor–Cu_2O composites with Cu_2O loadings of (a) 3.46 wt%, (b) 14.4 wt%, and (c) 29.7 wt%

Ullmann-type cross coupling of aryl halides with alcohols are one of the most important reactions for C–O bond formation in organic synthesis. The reaction is frequently used in the synthesis of pharmaceuticals, agrochemicals, and dyes. A variety of copper species, such as $[Cu(MeCN)_4]PF_6$, $(CuOTf)_2 \cdot C_6H_6$ (OTf = trifluoromethanesulfonate), $(CuOTf)_2 \cdot PhMe$, $[Cu(PPh_3)_3Br]$, $[Cu(MeCN)_4]PF_4$, CuI, and CuCl, have been reported as useful catalysts for this type of reaction. In addition to the copper species, many kinds of bases, including $CsCO_3$, K_2CO_3, KO^tBu, 4-dimethylaminopyridine (DMAP), and NaOMe/MeOH, have also been added to promote the reaction by neutralizing the co-product HX [23–25].

There are very few reports of C–O bond formation via Ullmann type cross coupling reactions catalyzed by Cu_2O catalysts in heterogeneous systems [12]. We tested the as-prepared TiO_2 precursor–Cu_2O composite (with 7.76 wt% of Cu_2O) as a catalyst for the cross coupling reaction of aryl halides with phenol. The reactions were carried out at 150 °C in DMF solution in air, and KOH was used as the base. After refluxing at 150 °C for 6 h, the yield reached 89% (Table 1, entry 1, based on ArI), indicating that the TiO_2 precursor–Cu_2O composite is quite active for this reaction. The small Cu_2O particle size, which leads to a large number of catalytic active sites, and the high stability of the Cu_2O nanoparticles are essential for the high catalytic activity. In a control experiment without any Cu_2O (Table 1, entry 5), no Ullmann reaction was observed, confirming that it cannot proceed without the Cu_2O species (Table 1, entry 5). Commercial Cu_2O particles showed much lower activity in this reaction due to their bulky size, and a yield of only 20% was observed after 6 h (Table 1, entry 4). Besides iodobenzene, both chlorobenzene and bromobenzene were also tested in the cross coupling reaction with phenol. After refluxing in DMF for 6 h, chlorobenzene did not give any product at all, whereas bromobenzene gave a 56% yield. Chlorobenzene and bromobenzene are known for their low reactivity in coupling reactions, and the 56% yield from bromobenzene is among the highest reported values for Ullmann type reactions of this material. In addition, DMSO and K_2CO_3 were also used as alternative solvent and base in control experiments (Table 1, entries 2 and 3). The observed

Table 1 Reactions of aryl halides with phenol under various conditions

Entry	ArX	Catalyst	Solvent	Base	Time (h)	Yield[a] (%)
1	ArI	TiO_2–Cu_2O	DMF	KOH	6	89
2	ArI	TiO_2–Cu_2O	DMSO	KOH	6	75
3	ArI	TiO_2–Cu_2O	DMF	K_2CO_3	6	40
4	ArI	Commercial Cu_2O	DMF	KOH	6	20
5	ArI	Blank	DMF	KOH	24	0
6	ArCl	TiO_2–Cu_2O	DMF	KOH	6	Trace
7	ArBr	TiO_2–Cu_2O	DMF	KOH	6	56
8	ArI	TiO_2–Cu_2O	DMF	KOH	6	90[b]

[a] Reaction conditions: 1 mmol of ArX, 1.2 mmol of phenol, 0.25 mmol of biphenyl (as internal standard), 2.4 mmol of base, 5 mL of solvent, 0.05 mmol of Cu_2O catalyst, 150 °C.
[b] The yield from the catalyst after being recycled five times

yields were lower than for DMF/KOH, showing that the solvent and the base both influence the reactivity of the system.

When the TiO_2 precursor–Cu_2O composite was recycled five times, it showed no loss of activity, with yields of around 90% in all five cycles as shown in Fig. 5(a). In general, the loss and the coalescence of particles during the catalytic process is the biggest problem with nanocatalysts, due to their small particle size (typically several nanometers). In order to overcome this problem, many nanocatalysts have been anchored on various solid supports to form composite structures. The Cu_2O nanocatalyst in the composite has a particle size of a few nanometers and is uniformly dispersed on the support surface (Fig. 1(b)). Such isolation and strong anchoring on the support prevent the aggregation of Cu_2O nanoparticles. A TEM image of the TiO_2 precursor–Cu_2O composite (with 7.76 wt% of Cu_2O), after recycling five times, is shown in Fig. 5(b). The Cu_2O nanoparticles dispersed on the TiO_2 precursor surface are clearly visible in Fig. 5(b) and the size of these particles is still around 3–4 nm, similar to the size in the fresh TiO_2 precursor–Cu_2O composite. This indicates that the structure of the composite did not change significantly after repeated runs. Other materials have not been used as the substrates for Cu_2O due to the difficulty in synthesis, but it will be very interesting if substrate effects can be studied.
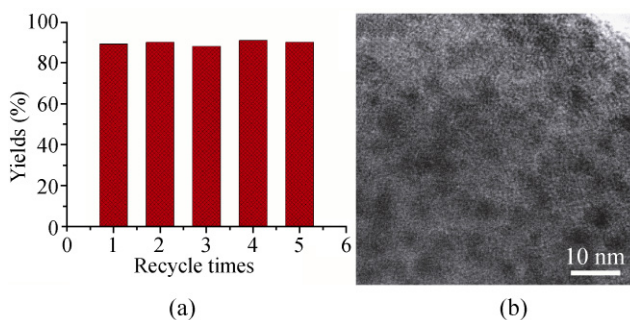
Figure 5 (a) Recycling results and (b) TEM image of the TiO_2 precursor–Cu_2O composite (with 7.76 wt% of Cu_2O) after five runs

In order to test the effect of Cu_2O loading on catalytic activity, four samples with loadings of 3.46 wt%, 7.76 wt%, 14.4 wt%, and 29.7 wt% of Cu_2O were tested in the time dependent cross coupling reaction between iodobenzene and phenol. The reaction conditions were kept the same in all four cases. After reaction for a specific time, aliquots of the reaction mixture were collected and analyzed by GC. Figure 6 shows the activity profiles of the four catalysts with different Cu_2O loadings in the cross coupling reaction between iodobenzene and phenol. The TiO_2 precursor–Cu_2O composite with 3.46 wt% of Cu_2O showed the highest activity, while the sample with 29.7 wt% of Cu_2O exhibited the lowest reaction rate. The yield decreased as the Cu_2O loading increased. Since the total amounts of Cu_2O used in these reactions were kept constant in all four experiments by using an
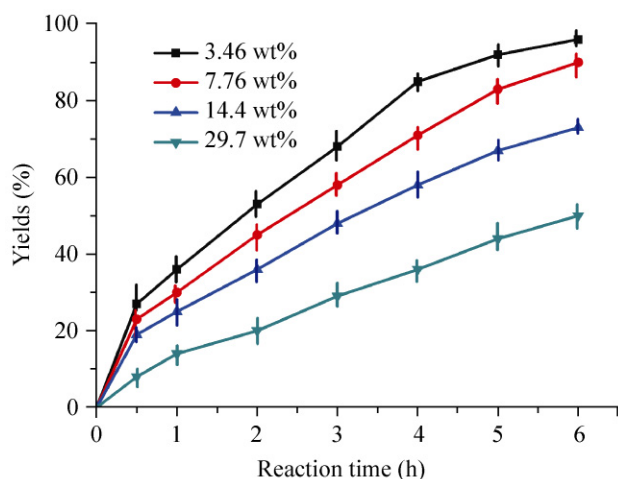
appropriate amount of the composite catalyst, the catalytic activity of the composite must be determined by the size of the Cu_2O nanoparticles. Smaller Cu_2O particles lead to more catalytically active sites on the catalyst surface. A similar trend has been observed in our previous work, where the catalytic activities of TiO_2 precursor–Pd catalysts for the Suzuki reaction were higher with lower Pd loadings. It will be very interesting if the shape effect of the Cu_2O particles can be studied. However, due to the difficulties in preparing Cu_2O particles with various regular shapes, such a study has not been possible to date.

4. Conclusions

We have produced composite catalysts with Cu_2O nanoparticles on the surface of hydroxyl group rich TiO_2 precursor spheres using an *in situ* loading method. Cu_2O nanoparticles were formed *in situ* by reduction of a $Cu(OH)_2$ colloid with the Sn^{2+} ions linked to the TiO_2 surface. The initially formed Cu_2O species became attached on the surface of the TiO_2 precursor and served as seeds for subsequent particle growth. The resulting Cu_2O nanoparticles are heat and air stable and evenly dispersed on the surface of the TiO_2 precursor. The as-prepared TiO_2 precursor–Cu_2O composite shows high catalytic activity for Ullmann type cross coupling reactions of aryl halides with phenol. The Cu_2O nanoparticles did not aggregate after five runs and the TiO_2 precursor–Cu_2O composite catalyst was recycled five times without loss of activity.

Acknowledgments

Figure 6 Activity profiles for the cross coupling reaction between iodobenzene and phenol catalyzed by TiO_2 precursor–Cu_2O composites with different Cu_2O loadings

References

[1] Corma, A.; Serna, P. Chemoselective hydrogenation of nitro compounds with supported gold catalysts. *Science* **2006**, *313*, 332–334.

[2] Enache, D. I.; Edwards, J. K.; Landon, P.; Solsona-Espriu, B.; Carley, A. F.; Herzing, A. A.; Watanabe, M.; Kiely, C. J.; Knight, D. W.; Hutchings, G. J. Solvent-free oxidation of primary alcohols to aldehydes using Au–Pd/TiO$_2$ catalysts. *Science* **2006**, *311*, 362–365.

[3] Hughes, M. D.; Xu, Y. -J.; Jenkins, P.; McMorn, P.; Landon, P.; Enache, D. I.; Carley, A. F.; Attard, G. A.; Hutchings, G. J.; King, F.; Stitt, E. H.; Johnston, P.; Griffin, K.; Kiely, C. J. Tunable gold catalysts for selective hydrocarbon oxidation under mild conditions. *Nature* **2005**, *437*, 1132–1135.

[4] Liang, H. -P.; Zhang, H. -M.; Hu, J. -S.; Guo, Y. -G.; Wan, L. -J.; Bai, C. -L. Pt hollow nanospheres: Facile synthesis and enhanced electrocatalysts. *Angew. Chem. Int. Ed.* **2004**, *43*, 1540–1543.

[5] Astruc, D.; Lu, F.; Aranzaes, J. R. Nanoparticles as recyclable catalysts: The frontier between homogeneous and heterogeneous catalysis. *Angew. Chem. Int. Ed.* **2005**, *44*, 7852–7872.

[6] Valden, M.; Lai, X.; Goodman, D. W. Onset of catalytic activity of gold clusters on titania with the appearance of nonmetallic properties. *Science* **1998**, *281*, 1647–1650.

[7] Huang, J.; Jiang, T.; Gao, H. -X.; Han, B. -X.; Liu, Z. -M.; Wu, W. -Z.; Chang, Y. -H.; Zhao, G. -Y. Pd nanoparticles immobilized on molecular sieves by ionic liquids: Hetero-geneous catalysts for solvent-free hydrogenation. *Angew. Chem. Int. Ed.* **2004**, *43*, 1397–1399.

[8] Zhang, J. -Y.; Zhu, H. -L.; Zheng, S. -K.; Pan, F.; Wang, T. -M. TiO$_2$ film/Cu$_2$O microgrid heterojunction with photocatalytic activity under solar light irradiation. *ACS Appl. Mater. Interf.* **2009**, *1*, 2111–2114.

[9] Bessekhouad, Y.; Robert, D.; Weber, J. V. Photocatalytic activity of Cu$_2$O/TiO$_2$, Bi$_2$O$_3$/TiO$_2$ and ZnMn$_2$O$_4$/TiO$_2$ heterojunctions. *Catal. Today* **2005**, *101*, 315–321.

[10] Ho, J. -Y.; Huang, M. H. Synthesis of submicrometer-sized Cu$_2$O crystals with morphological evolution from cubic to hexapod structures and their comparative photocatalytic activity. *J. Phys. Chem. C* **2009**, *113*, 14159–14164.

[11] Le, D.; Stolbov, S.; Rahman, T. S. Reactivity of the Cu$_2$O(100) surface: Insights from first principles calculations. *Surf. Sci.* **2009**, *603*, 1637–1645.

[12] Kim, J. Y.; Park, J. C.; Kim, A.; Kim, A. Y.; Lee, H. J.; Song, H.; Park, K. H. Cu$_2$O Nanocube-catalyzed cross-coupling of aryl halides with phenols via Ullmann coupling. *Eur. J. Inorg. Chem.* **2009**, *2009*, 4219–4223.

[13] Son, S. U.; Park, I. K.; Park, J.; Hyeon, T. Synthesis of Cu$_2$O coated Cu nanoparticles and their successful applications to Ullmann-type amination coupling reactions of aryl chlorides. *Chem. Commun.* **2004**, 778–779.

[14] Gou, L. F.; Murphy, C. J. Solution-phase synthesis of Cu$_2$O nanocubes. *Nano Lett.* **2002**, *3*, 231–234.

[15] Wang, D. B.; Mo, M. S.; Yu, D. B.; Xu, L. Q.; Li, F. Q.; Qian, Y. T. Large-scale growth and shape evolution of Cu$_2$O cubes. *Cryst. Growth Des.* **2003**, *3*, 717–720.

[16] Gou, L. F.; Murphy, C. J. Controlling the size of Cu$_2$O nanocubes from 200 to 25 nm. *J. Mater. Chem.* **2004**, *14*, 735–738.

[17] Xu, H. L.; Wang, W. Z. Template synthesis of multishelled Cu$_2$O hollow spheres with a single-crystalline shell wall. *Angew. Chem. Int. Ed.* **2007**, *46*, 1489–1492.

[18] Xu, L.; Jiang, L. P.; Zhu, J. J. Sonochemical synthesis and photocatalysis of porous Cu$_2$O nanospheres with controllable structures. *Nanotechnology* **2009**, *20*, 045605.

[19] Hung, L. I.; Tsung, C. K.; Huang, W. Y.; Yang, P. D. Room-temperature formation of hollow Cu$_2$O nanoparticles. *Adv. Mater.* **2010**, *22*, 1910–1914.

[20] Kuo, C. H.; Hua, T. E.; Huang, M. H. Au nanocrystal-directed growth of Au–Cu$_2$O core–shell heterostructures with precise morphological control. *J. Am. Chem. Soc.* **2009**, *131*, 17871–17878.

[21] Zhong, L. S.; Hu, J. S.; Cui, Z. M.; Wan, L. J.; Song, W. G. *In-situ* loading of noble metal nanoparticles on hydroxyl-group-rich titania precursor and their catalytic applications. *Chem. Mater.* **2007**, *19*, 4557–4562.

[22] Zhong, L. S.; Hu, J. S.; Wan, L. J.; Song, W. G. Facile synthesis of nanoporous anatase spheres and their environmental applications. *Chem. Commun.* **2008**, 1184–1186.

[23] Beletskaya, I. P.; Cheprakov, A. V. Copper in cross-coupling reactions: The post-Ullmann chemistry. *Coord. Chem. Rev.* **2004**, *248*, 2337–2364.

[24] Ley, S. V.; Thomas, A. W. Modern synthetic methods for copper-mediated C(aryl)–O, C(aryl)–N, and C(aryl)–S bond formation. *Angew. Chem. Int. Ed.* **2003**, *42*, 5400–5449.

[25] Ma, D. W.; Cai, Q. *N*, *N*-Dimethyl glycine-promoted Ullmann coupling reaction of phenols and aryl halides. *Org. Lett.* **2003**, *5*, 3799–3802.